Spatially Correlated Reconfigurable Intelligent Surfaces-Aided Cell-Free Massive MIMO Systems

Enyu Shi, Jiayi Zhang, *Senior Member, IEEE*, Ruisi He, *Senior Member, IEEE*, Huiying Jiao, Zhiqin Wang, Bo Ai, *Fellow, IEEE*, and Derrick Wing Kwan Ng, *Fellow, IEEE*

***Abstract*—Reconfigurable intelligent surfaces (RISs) and cell-free (CF) massive multiple-input multiple-output (MIMO) are two promising technologies for realizing beyond-fifth generation (5G) networks. In this paper, we study the uplink spectral efficiency (SE) of a practical spatially correlated RISs-aided CF massive MIMO system over Rician fading channels. Specifically, we derive the closed-form expression for characterizing the uplink SE of the system, which shows that increasing the number of RIS elements can improve the system performance. Moreover, the results unveil that the spatial correlation of RIS has a significant impact on the system while leading to the best performance gain at a half wavelength spacing. Finally, the accuracy of our analytical results are verified by Monte-Carlo simulations.**

***Index Terms*—Reconfigurable intelligent surface, cell-free massive MIMO, spatial correlation, spectral efficiency.**

I. Introduction

Reconfigurable intelligent surface (RIS) has recently emerged as a promising new paradigm to establish smart and reconfigurable wireless channels/radio propagation environment for beyond-5G (B5G) wireless communication systems [1], [2]. For instance, in [3], with massive reflective and refractive elements, RIS can realize effective passive beamforming by altering the phase of the reflected impinging signal. It has the advantages of easy deployment, low power, and low cost. Meanwhile, cell-free (CF) massive MIMO is a network architecture where a large number of access points (APs) are deployed in the coverage to serve users. It is regarded as one of the most promising technologies for B5G wireless communication [4]. In practice, CF massive MIMO can support a large number of users and improve the quality of communication by shortening the distances between users and the base stations. More importantly, CF massive MIMO can effectively exploit the spatial degrees of freedom which facilitates interference management among users [5]–[8].

Recently, a number of studies have focused on how to jointly exploit the advantages of RIS and cell-free massive MIMO to improve communication performance [9]. For example, some works have considered a single RIS-aided system [10], [11]. It was shown that such a system can greatly enhance the link quality and coverage, owing to the capability in shaping favorable propagation and the dispersed distribution of RISs. Also, in [12], the authors proposed a new channel estimation method for RIS-aided CF communications, which can estimate all channels by switching each element in turn. Besides, in [13], the authors deployed RISs to assist CF massive MIMO and proposed an iterative algorithm to address the system sum-rate optimization problem. However, none of the aforementioned studies considered the impact of spatial correlation of RIS on the system performance. Indeed, the size of a RIS element is of subwavelength such that spatial correlations among RIS elements naturally exist. Therefore, the spatial correlation channel model of RIS represented by the sinc function was proposed in [14]. Specifically, the authors showed that the characteristics of spatial correlation channels can be manipulated by adjusting the spacing among RIS elements. Also, in [15], the authors proposed an aggregated channel estimation method and considered the performance of a CF system assisted by a single spatial correlation RIS. However, the performance of the RIS-aided cell-free massive MIMO system under spatially correlated channels has not been fully studied, yet.

In this work, motivated by the above consideration, we investigate the uplink performance of RISs-aided CF massive MIMO systems under spatially correlated channels. More specifically, we propose the minimum mean square error (MMSE) channel estimation scheme to estimate the channels between user equipments (UEs), RISs, and APs by switching elements in turn. Then, the closed-form expression for the uplink spectral efficiency (SE) of the RISs-aided CF massive MIMO systems is derived. The results show that increasing the number of RISs or the number of elements of each RIS can improve the system performance, especially when the direct links are blocked with a high probability. Moreover, the spatial correlation of RIS has a significant impact on RISs-aided CF massive MIMO systems while leading to the best performance gain at a half wavelength spacing.

II. System Model

As illustrated in Fig. 1, we consider a RISs-aided CF massive MIMO system with M APs, K UEs, and T_r RISs. All APs and UEs are equipped with a single-antenna and each RIS has L reflective elements. To fully exploit the spatial characteristic of CF, we assume that each deployed RIS is close to one AP. As such, through RIS beamforming, it is guaranteed that the beam reflected from the RIS can be effectively focused on the desired AP [10], [16]. In this scenario, the interference caused by other RISs is weak enough to be ignored. As introduced in [2], [3], we model the re-established RIS-AP and UE-RIS channels by Rician fading. Besides, there is no direct path between UEs and APs

Manuscript received 31 March 2022; accepted 11 May 2022. Date of publication 19 May 2022; date of current version 15 August 2022. This work was supported in part by the National Key R&D Program of China under Grant 2020YFB1806903, in part by the National Natural Science Foundation of China under Grant 61971027, in part by the Beijing Natural Science Foundation under Grant L202013, and in part by the Frontiers Science Center for Smart High-speed Railway System. The work of D. W. K. Ng was supported by the UNSW Digital Grid Futures Institute, UNSW, Sydney, under a cross-disciplinary fund scheme and by the Australian Research Council's Discovery Project under Grant DP210102169. The review of this article was coordinated by Prof. Zhu Han. *(Corresponding authors: Zhiqin Wang; Jiayi Zhang.)*

Enyu Shi and Jiayi Zhang are with the School of Electronics and Information Engineering, Beijing Jiaotong University, Beijing 100044, China, and also with the Frontiers Science Center for Smart High-speed Railway System, Beijing Jiaotong University, Beijing 100044, China (e-mail: 21111047@bjtu.edu.cn; jiayizhang@bjtu.edu.cn).

Ruisi He is with the State Key Laboratory of Rail Traffic Control and Safety, Beijing Jiaotong University, Beijing 100044, China (e-mail: ruisi.he@bjtu.edu.cn).

Huiying Jiao and Zhiqin Wang are with the China Academy of Information and Communications Technology, Beijing 100191, China (e-mail: jiaohuiying@caict.ac.cn; zhiqin.wang@caict.ac.cn).

Bo Ai is with the Frontiers Science Center for Smart High-speed Railway System, Beijing Jiaotong University, Beijing 100044, China, with the State Key Laboratory of Rail Traffic Control and Safety, Beijing Jiaotong University, Beijing 100044, China, with the Henan Joint International Research Laboratory of Intelligent Networking and Data Analysis, Zhengzhou University, Zhengzhou 450001, China, and also with the Research Center of Networks and Communications, Peng Cheng Laboratory, Shenzhen 518000, China (e-mail: boai@bjtu.edu.cn).

Derrick Wing Kwan Ng is with the School of Electrical Engineering and Telecommunications, University of New South Wales, Kensington, NSW 2033, Australia (e-mail: w.k.ng@unsw.edu.au).

Digital Object Identifier 10.1109/TVT.2022.3175459

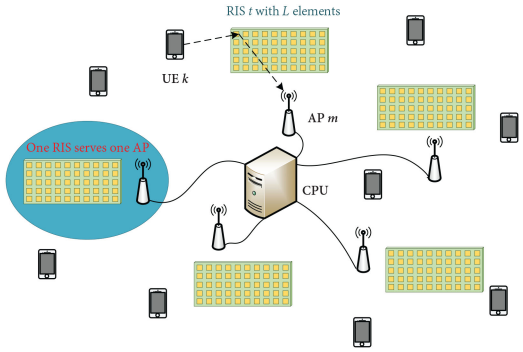

Fig. 1. An RISs-aided CF massive MIMO system.

and the transmission environment needs to be enhanced through RIS to realize efficient communication [17]. Note that we consider multiple RISs and adopt the Rician fading channel models, which introduces a generalized framework compared with [15]. The total cascaded uplink channel between UE $k \in \{1, \ldots, K\}$ and AP $m \in \{1, \ldots, M\}$ is given by

$$g_{mtlk} = g_{tlm} e^{j\theta_{tl}} g_{ktl}, \tag{1}$$

where g_{tlm} denotes the channel from element $l \in \{1, \ldots, L\}$ in RIS $t \in \{1, \ldots, T_r\}$ to AP m whereas g_{ktl} is the channel from UE k to element l of RIS t. We model the two channels as $g_{tlm} = \bar{g}_{tlm} + \tilde{g}_{tlm}$ and $g_{ktl} = \bar{g}_{ktl} + \tilde{g}_{ktl}$, respectively, where $\tilde{g}_{tlm} \sim \mathcal{CN}(0, \beta_{tlm})$ and $\tilde{g}_{ktl} \sim \mathcal{CN}(0, \beta_{ktl})$ are the corresponding NLoS components, while $\bar{g}_{tlm}$ and $\bar{g}_{ktl}$ are the corresponding LoS components. β_{tlm} and β_{ktl} denote the large-scale fading coefficients of element l of RIS t to AP m and UE k, respectively. Moreover, $\theta_{tl} \in [0, 2\pi]$ is the phase shift introduced by element l of RIS t. The cascaded uplink channel from UE k to AP m through element l of RIS t is given as

$$\begin{aligned} g_{mtlk} &= g_{tlm} e^{j\theta_{tl}} g_{ktl} \\ &= \underbrace{\bar{g}_{tlm} \bar{g}_{ktl} e^{j\theta_{tl}}}_{\bar{g}_{mtlk}} + \underbrace{(\bar{g}_{tlm} \tilde{g}_{ktl} + \tilde{g}_{tlm} \bar{g}_{ktl} + \tilde{g}_{tlm} \tilde{g}_{ktl}) e^{j\theta_{tl}}}_{\tilde{g}_{mtlk}} \\ &= \bar{g}_{mtlk} + \tilde{g}_{mtlk}. \end{aligned} \tag{2}$$

Note that due to the assumption that the LoS component is known as a priori and changes slowly across time, the information of $\bar{g}_{mtlk}$ is available, i.e., the first term of (2). The Rician κ-factor and the large-scale fading coefficients vary depending on the locations of UEs and APs. Moreover, the additional phase-shift $e^{j\varphi_{mtlk}}$ exists on the LoS component as $\bar{g}_{mtlk} e^{j\varphi_{mtlk}}$. We assume that the magnitude of RIS phase shift in (1) is $|e^{j\theta}|^2 = 1$ and $\theta = \pi/4$ [15], [18]. Therefore, we have

$$\beta_{mtlk} = \mathbb{E}\left\{|\bar{g}_{mtlk}|^2\right\} = \beta_{ktl} |\bar{g}_{tlm}|^2 + \beta_{tlm} |\bar{g}_{ktl}|^2 + \beta_{tlm} \beta_{ktl}, \tag{3}$$

where $E\{\cdot\}$ denotes the expectation of a random variable.

Considering the spatial correlation of RIS elements, with isotropic scattering in the half-space in front of the RIS [14], the spatial correlation matrix $\mathbf{R}$ of each RIS has elements $[\mathbf{R}]_{p,q} = \mathrm{sinc}(2\|d_{p,q}\|/\lambda)$ with $p, q = 1, 2, \ldots, L$, where $\mathrm{sinc}(x) = \sin(\pi x)/(\pi x)$. Variable $d_{p,q} = u_p - u_q$ represents the spacing between elements p and q, and the wavelength is represented by λ. Furthermore, we have $\mathrm{u}_p = [0, \mod(p-1, N_\mathrm{H}) d_\mathrm{H}, \lfloor (p-1)/N_\mathrm{H} \rfloor d_\mathrm{V}]^T$, where N_H and N_V denote the number of elements per row and per column, respectively, such that $L = N_\mathrm{H} \times N_\mathrm{V}$. $|\cdot|$ and $\|\cdot\|$ denote the absolute value and Euclidean norm. $\mathrm{mod}(\cdot, \cdot)$ is the modulus operation and $\lfloor \cdot \rfloor$ denotes the truncated argument. d_H and d_V are the horizontal width and the vertical height of each element, respectively. The superscripts $(\cdot)^*$, $(\cdot)^T$, and $(\cdot)^H$ denote the conjugate, transpose, and conjugate-transpose, respectively.

A. Uplink Channel Estimation

We adopt the time-division duplex (TDD) transmission protocol, where the uplink channels are estimated by each AP [19], [20]. With the method developed in [12], in every subtime slot, element l on RIS t is on, while the other elements are off. We denote τ_c as the length of each coherence block and we adopt an orthogonal pilot sequence τ_p to estimate the channel and $\tau_b = \tau_c - \tau_p$ is exploited for data transmission. $\boldsymbol{\phi}_k \in \mathbb{C}^{\tau_p \times 1}$ denotes the pilot sequence of UE k and satisfies $\|\boldsymbol{\phi}_k\|^2 = \tau_p$. Let $\mathcal{P}_k$ denote the index subset of UEs which adopts the same pilot sequence as UE k including itself. The received signal $\mathbf{y}^p_{mtl} \in \mathbb{C}^{\tau_p \times 1}$ at AP m can be expressed as

$$\mathbf{y}^p_{mtl} = \sum_{k=1}^{K} \sqrt{\hat{p}_k} g_{mtlk} \boldsymbol{\phi}_k + \mathbf{n}^p_{mtl}, \tag{4}$$

where $\hat{p}_k$ denotes the transmit power from UE k, $\mathbf{n}^p_{mtl} \sim \mathcal{CN}(0, \sigma^2 \mathbf{I}_{\tau_p})$ is the additive noise, and σ^2 is the noise power. Then, AP m multiplies the received signal by $\boldsymbol{\phi}^H_k$ to obtain the estimated channel as

$$\begin{aligned} y^p_{mtlk} &= \boldsymbol{\phi}^H_k \mathbf{y}^p_{mtl} \\ &= \sqrt{\hat{p}_k} \tau_p g_{mtlk} + \sum_{u \in \mathcal{P}_k \setminus \{k\}} \sqrt{\hat{p}_u} \tau_p g_{mtlu} + \boldsymbol{\phi}^H_k \mathbf{n}^p_{mtl}. \end{aligned} \tag{5}$$

Based on (5), after all elements have been switched on and off in turn, AP m obtains signal $\mathbf{y}^p_{mtk} \triangleq [y^p_{mt1k}, y^p_{mt2k}, \ldots, y^p_{mtLk}]^T$. Since the channel statistics $\bar{g}_{mtlk}$, β_{mtlk} are known to AP m, we adopt the MMSE channel estimation method, as reported in [15], [21], to estimate the channel $\mathbf{g}_{mtk}$ as

$$\hat{\mathbf{g}}_{mtk} = \bar{\mathbf{g}}_{mtk} e^{j\varphi_{mtk}} + \sqrt{\hat{p}_k} \mathbf{R}_{mtk} \boldsymbol{\Lambda}^{-1}_{mtk} \left(\mathbf{y}^p_{mtk} - \bar{\mathbf{y}}^p_{mtk}\right), \tag{6}$$

where the channels $\bar{\mathbf{g}}_{mtk} \triangleq [\bar{g}_{mt1k}\rho, \bar{g}_{mt2k}\rho, \ldots, \bar{g}_{mtLk}\rho]^T$, the matrix $\mathbf{R}_{mtk} = \mathrm{diag}(\beta_{mt1k}\rho, \beta_{mt2k}\rho, \ldots, \beta_{mtLk}\rho)$, the correlation coefficient $\rho = \mathrm{tr}(\mathbf{R}^2)/L$, the direct component part $\bar{\mathbf{y}}^p_{mtk} = \sum_{u \in \mathcal{P}_k} \sqrt{\hat{p}_u} \tau_p \bar{\mathbf{g}}_{mtu}$, and $\boldsymbol{\Lambda}^{-1}_{mtk} = \sum_{u \in \mathcal{P}_k} \sqrt{\hat{p}_u} \tau_p \mathbf{R}_{mtu} + \sigma^2 \mathbf{I}$. $\mathrm{tr}(\cdot)$ is the trace operator. Note that $\mathbf{y}^p_{mtk}$ and $\bar{\mathbf{y}}^p_{mtk}$ vary in each coherence block, so the channel estimate $\hat{\mathbf{g}}_{mtk}$ and the estimation error $\tilde{\mathbf{g}}_{mtk} = \mathbf{g}_{mtk} - \hat{\mathbf{g}}_{mtk}$ are independent random variables with [22]. The mean and variance of $\hat{\mathbf{g}}_{mtk}$ are $\bar{\mathbf{g}}_{mtk}$ and $\hat{p}_k \tau_p \boldsymbol{\Omega}_{mtk}$, respectively. Here, $\boldsymbol{\Omega}_{mtk} = \mathbf{R}_{mtk} \boldsymbol{\Lambda}^{-1}_{mtk} \mathbf{R}_{mtk}$ and the covariance matrix of $\tilde{\mathbf{g}}_{mtk}$ can be obtained as $\mathbf{C}_{mtk} = \mathbf{R}_{mtk} - \hat{p}_k \tau_p \boldsymbol{\Omega}_{mtk}$. The mean-squared error is $\mathrm{MSE} = \mathbb{E}\{|\mathbf{g}_{mtk} - \hat{\mathbf{g}}_{mtk}|^2\} = \mathbf{C}_{mtk}$. Note that the aggregated channel estimation method reduces the signaling overhead at the expense of the complexity [15], while our method has a lower complexity with the increased overhead.

Remark 1: Note that when we estimate the channel, the elements switch on/off in turn, so there is no RIS elements correlation in (5). While AP know the correlation matrix $\mathbf{R}$, because it only depends on the structure of RIS. On the other hand, since the positions of RISs and APs are fixed, the channel of RIS-AP can be obtained accurately, which can be well captured by some channel coefficients. Therefore, it is not necessary to consider the correlation caused by the common channel from AP n to RIS t.

B. Uplink Data Transmission

In this subsection, we consider the uplink data transmission, where all UEs send τ_b duration of uplink data to the APs in each coherence block. In other words, each AP can receive the signal from all UEs. Then, the received signal at AP m is given by

$$y_m = \sum_{k=1}^{K}\sum_{l=1}^{L} g_{mtlk} s_k + n_m, \tag{7}$$

where $s_k \sim \mathcal{CN}(0, p_k)$ is the uplink signal of UE k with power $p_k = \mathbb{E}\{|s_k|^2\}$ and $n_m \sim \mathcal{CN}(0,1)$ is the noise at AP m. AP m utilizes the combined channel estimates, $v_{mtk} = \sum_{l=1}^{L} \hat{g}_{mtlk}$, to detect the signal of UE k and the estimate of s_k is derived by

$$\begin{aligned}\tilde{s}_{m,k} &= v_{mtk}^* y_m \\ &= v_{mtk}^* g_{mtk} s_k + \sum_{u=1,u\neq k}^{K} v_{mtk}^* g_{mtu} s_u + v_{mtk}^* n_m. \end{aligned}\tag{8}$$

where $g_{mtk} = \sum_{l=1}^{L} g_{mtlk}$. We assume that there is a central processing unit (CPU) that only receives $\tilde{s}_{m,k}$ from the APs for joint processing. At the CPU, all APs signals can be written as

$$\tilde{s}_k = \mathbf{v}_{tk}^H \mathbf{g}_{tk} s_k + \sum_{u=1,u\neq k}^{K} \mathbf{v}_{tk}^H \mathbf{g}_{tu} s_u + n_k, \tag{9}$$

where the combining vector $\mathbf{v}_{tk} = [v_{1tk}, v_{2tk}, \ldots, v_{Mtk}]^T$, $\mathbf{g}_{tk} = [g_{1tk}, g_{2tk}, \ldots, g_{Mtk}]^T$, and $n_k = \sum_{m=1}^{M} v_{mtk}^* n_m$.

III. Spectral Efficiency Analysis

In this section, we investigate the uplink performance of RISs-aided CF massive MIMO systems and explore the impact of correlation and the number of RIS elements. Based on (9), the uplink ergodic achievable rate of UE k is lower bounded using the use-and-then-forget (UatF) bound as

$$\mathrm{SE}_k = \frac{\tau_b}{\tau_c}\log_2\left(1+\gamma_k\right), \tag{10}$$

where the uplink effective SINR γ_k of UE k is given as [22]

$$\gamma_k = \frac{p_k\left|\mathbb{E}\left\{\mathbf{v}_{tk}^H\mathbf{g}_{tk}\right\}\right|^2}{\sum_{u=1}^{K} p_u \mathbb{E}\left\{\left|\mathbf{v}_{tk}^H\mathbf{g}_{tu}\right|^2\right\} - p_k\left|\mathbb{E}\{\mathbf{v}_{tk}^H\mathbf{g}_{tk}\}\right|^2 + \sigma^2\mathbb{E}\left\{\left\|\mathbf{v}_{tk}\right\|^2\right\}}. \tag{11}$$

The maximum-ratio (MR) combining has lower complexity than MMSE and its closed-form structure facilitates performance analysis [22]. In the following sections, we apply MR combining for $\mathbf{v}_{tk}$ to compute γ_k based on the MMSE channel estimator, which yields

$$\begin{aligned}\mathbb{E}\left\{v_{mtk}^H g_{mtk}\right\} &= \hat{p}_k\tau_p \mathrm{tr}(\mathbf{R}_{mtk}\boldsymbol{\Lambda}_{mtk}^{-1}\mathbf{R}_{mtk}) + \left\|\bar{\mathbf{g}}_{mtk}\right\|^2 \\ &= \hat{p}_k\tau_p\mathrm{tr}(\boldsymbol{\Omega}_{mtk}) + \left\|\bar{\mathbf{g}}_{mtk}\right\|^2. \end{aligned}\tag{12}$$

Based on (12), we have

$$\mathbb{E}\{\mathbf{v}_{tk}^H\mathbf{g}_{tk}\} = \hat{p}_k\tau_p\mathrm{tr}\left(\boldsymbol{\Xi}_k\right) + \mathrm{tr}\left(\bar{\mathbf{G}}_k\right), \tag{13}$$

where $\boldsymbol{\Xi}_k = \mathrm{diag}(\mathrm{tr}(\boldsymbol{\Omega}_{1tk}), \mathrm{tr}(\boldsymbol{\Omega}_{2tk}), \ldots, \mathrm{tr}(\boldsymbol{\Omega}_{Mtk}))$ and $\bar{\mathbf{G}}_k = \mathrm{diag}(\|\bar{\mathbf{g}}_{1tk}\|^2, \|\bar{\mathbf{g}}_{2tk}\|^2, \ldots, \|\bar{\mathbf{g}}_{Mtk}\|^2)$. Then the term of noise is given by

$$\mathbb{E}\left\{\left\|\mathbf{v}_{tk}\right\|^2\right\} = \hat{p}_k\tau_p\mathrm{tr}\left(\boldsymbol{\Xi}_k\right) + \mathrm{tr}\left(\bar{\mathbf{G}}_k\right). \tag{14}$$

Note that the expectation of the estimation error $\tilde{\mathbf{g}}_{tk}$ times $\hat{\mathbf{g}}_{tk}^H$ is zero, so (13) and (14) are identical. Also, the first term of the denominator can be expressed as

$$\mathbb{E}\left\{\left|\mathbf{v}_{tk}^H\mathbf{g}_{tu}\right|^2\right\} = \sum_{m=1}^{M}\sum_{n=1}^{M}\mathbb{E}\left\{\left(v_{mtk}^H g_{mtu}\right)^H\left(v_{ntk}^H g_{ntu}\right)\right\}. \tag{15}$$

We know that the channel estimates at different APs are independent. In the first case, for $m \neq n$ and $u \notin \mathcal{P}_k$, we have $\mathbb{E}\{(v_{mtk}^H g_{mtu})^H (v_{ntk}^H g_{ntu})\} = 0$, as v_{ntk}^H and g_{ntu} both have zero mean and they are statistically independent. When $u \in \mathcal{P}_k$, it can be divided into two cases: $u = k$ and $u \neq k$. For the first subcase, we have

$$\begin{aligned}\mathbb{E}\left\{\left|\mathbf{v}_{tk}^H\mathbf{g}_{tk}\right|^2\right\} &= \hat{p}_k\tau_p\mathrm{tr}\left(\boldsymbol{\Sigma}_k\boldsymbol{\Xi}_k\right) + \mathrm{tr}\left(\bar{\mathbf{G}}_k^H\bar{\mathbf{G}}_k\right) \\ &\quad + \mathrm{tr}\left(\boldsymbol{\Sigma}_k\bar{\mathbf{G}}_k\right) + \hat{p}_k^2\tau_p^2\mathrm{tr}\left(\boldsymbol{\Xi}_k^H\boldsymbol{\Xi}_k\right) \\ &\quad + 3\hat{p}_k\tau_p\mathrm{tr}\left(\bar{\mathbf{G}}_k\boldsymbol{\Xi}_k\right), \end{aligned}\tag{16}$$

where $\boldsymbol{\Sigma}_k = \mathrm{diag}(\mathrm{tr}(\mathbf{R}_{1tk}), \mathrm{tr}(\mathbf{R}_{2tk}), \ldots, \mathrm{tr}(\mathbf{R}_{Mtk}))$. For the second subcase, we have

$$\begin{aligned}\mathbb{E}\left\{\left|\mathbf{v}_{tk}^H\mathbf{g}_{tu}\right|^2\right\} &= \hat{p}_k\tau_p\mathrm{tr}\left(\boldsymbol{\Sigma}_u\boldsymbol{\Xi}_k\right) + \mathrm{tr}\left(\bar{\mathbf{G}}_k^H\bar{\mathbf{G}}_u\right) + \mathrm{tr}\left(\boldsymbol{\Sigma}_u\bar{\mathbf{G}}_k\right) \\ &\quad + \hat{p}_k\tau_p\mathrm{tr}\left(\boldsymbol{\Xi}_k\bar{\mathbf{G}}_u\right) + \hat{p}_k\hat{p}_u\tau_p^2\left|\mathrm{tr}\left(\boldsymbol{\Sigma}_u\boldsymbol{\Upsilon}_k\boldsymbol{\Sigma}_k\right)\right|^2 \\ &\quad + 2\sqrt{\hat{p}_k\hat{p}_u}\tau_p\mathbf{Re}\left\{\mathrm{tr}\left(\boldsymbol{\Sigma}_u\boldsymbol{\Upsilon}_k\boldsymbol{\Sigma}_k\right)\bar{\mathbf{g}}_{tu}^H\bar{\mathbf{g}}_{tk}\right\}, \end{aligned}\tag{17}$$

where $\boldsymbol{\Upsilon}_k = \mathrm{diag}(\boldsymbol{\Lambda}_{1tk}^{-1}, \boldsymbol{\Lambda}_{2tk}^{-1}, \ldots, \boldsymbol{\Lambda}_{Mtk}^{-1})$ and the vector $\bar{\mathbf{g}}_{tk}^H = [\bar{\mathbf{g}}_{1tk}, \bar{\mathbf{g}}_{2tk}, \ldots, \bar{\mathbf{g}}_{Mtk}]^T$. Combining the above results and substitute them into (13), γ_k is given in (18) shown at the bottom of this page, where $\zeta_{ku}^{(1)}$ and $\zeta_{ku}^{(2)}$ are given by

$$\begin{aligned}\zeta_{ku}^{(1)} &= p_k\tau_p\mathrm{tr}\left(\boldsymbol{\Sigma}_u\boldsymbol{\Xi}_k\right) + p_k\tau_p\mathrm{tr}\left(\boldsymbol{\Xi}_k\bar{\mathbf{G}}_u\right) \\ &\quad + \mathrm{tr}\left(\boldsymbol{\Sigma}_u\bar{\mathbf{G}}_k\right) + \mathrm{tr}\left(\bar{\mathbf{G}}_k^H\bar{\mathbf{G}}_u\right), \end{aligned}\tag{19}$$

$$\begin{aligned}\zeta_{ku}^{(2)} &= p_k p_u\tau_p^2\left|\mathrm{tr}\left(\boldsymbol{\Sigma}_u\boldsymbol{\Upsilon}_k\boldsymbol{\Sigma}_k\right)\right|^2 \\ &\quad + 2\sqrt{p_k p_u}\tau_p\mathbf{Re}\left\{\mathrm{tr}\left(\boldsymbol{\Sigma}_u\boldsymbol{\Upsilon}_k\boldsymbol{\Sigma}_k\right)\bar{\mathbf{g}}_{tu}^H\bar{\mathbf{g}}_{tk}\right\}, \end{aligned}\tag{20}$$

respectively, which denote the non-coherent interference and the coherent interference terms, respectively. We note that in (18), $\mathbf{R}$ exists in the denominator $\boldsymbol{\Xi}_k$. Due to the characteristics of the sinc function, the correlations among RIS elements have a negative impact on SE. Note that compared with [23], we introduce the RIS assistance and considered the spatial correlation of RIS elements.

Proof: The proof is given in Appendix A. ■

$$\gamma_k = \frac{p_k\left|p_k\tau_p\mathrm{tr}\left(\boldsymbol{\Xi}_k\right) + \mathrm{tr}\left(\bar{\mathbf{G}}_k\right)\right|^2}{\sum_{u=1}^{K} p_u\zeta_{ku}^{(1)} + \sum_{u\in\mathcal{P}_k\setminus\{k\}} p_u\zeta_{ku}^{(2)} - p_k\mathrm{tr}\left(\bar{\mathbf{G}}_k\right)^2 + \sigma^2\left(p_k\tau_p\mathrm{tr}\left(\boldsymbol{\Xi}_k\right) + \mathrm{tr}\left(\bar{\mathbf{G}}_k\right)\right)}. \tag{18}$$

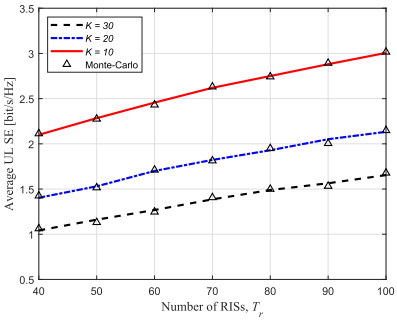

Fig. 2. Average SE against different number of RISs T_r with different number of UEs ($K = [10, 20, 30]$, $L = 4$, $d_{\mathrm{V}} = \frac{1}{2}\lambda$).

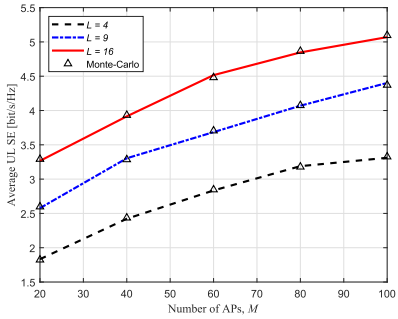

Fig. 3. Average SE against different number of APs M with different number of RIS elements ($L = [4, 9, 16]$, $K = 10$, $d_{\mathrm{V}} = \frac{1}{2}\lambda$).

IV. Numerical Results and Discussion

In this section, the derived SE expression of a RISs-aided CF massive MIMO systems is validated and evaluated by simulation results. We assume that the APs and the UEs are uniformly distributed in a 1×1 km^2 square area. The pathloss is computed by the COST 321 Walfish-Ikegami model for micro-cells in [15] with AP height 12.5 m and UE height 1.5 m, then the pathloss is modeled as

$$\beta_{tk}\,[\mathrm{dB}] = -30.18 - 26\log_{10}\left(\frac{d}{1\,\mathrm{m}}\right) + F_{tk}, \tag{21}$$

where d denotes the corresponding distance between AP, UE, and RIS. The Rician κ-factor can be expressed as $\kappa = 10^{1.3-0.003\,d}$. We consider the correlated shadow fading as in [24] with $F_{tk} = \sqrt{\delta_f}a_t + \sqrt{1-\delta_f}b_k$, where $a_t \sim \mathcal{N}(0,\delta_{sf}^2)$ and $b_k \sim \mathcal{N}(0,\delta_{sf}^2)$ are independent random variables and δ_f is the shadow fading parameter. The covariance functions a_t and b_k are given as $\mathbb{E}\{a_t a_{t'}\} = 2^{-\frac{d_{tt'}}{d_{dc}}}$ and $\mathbb{E}\{b_k b_{k'}\} = 2^{-\frac{d_{kk'}}{d_{dc}}}$, where $d_{tt'}$ and $d_{kk'}$ are the geographical distances between RIS t-RIS t' and UE k-UE k', respectively, d_{dc} is the decorrelation distance depending on the environment. As the distance between RIS and AP is less than 10 m, the pathloss is set as $\beta_{mt}[\mathrm{dB}] = -81.2$. Let $\delta_f = 0.5$, $d_{dc} = 100$ m, and $\delta_{sf} = 8$ in our paper. The large-scale coefficients are given by $\bar{g}_{tk} = \sqrt{\kappa_{tk}/(\kappa_{tk}+1)}\sqrt{\beta_{tk}}$, $\beta_{tk}^{\mathrm{NLOS}} = \beta_{tk}/(\kappa_{tk}+1)$ which can be estimated by exploiting the distance information [14], [16].

In addition, the coefficients between each AP and the corresponding RIS can be obtained in the same way. One RIS serves one AP, i.e., $M = T_r$. All the UEs transmit with power $p_k = 200$ mW and the receive noise power is $\sigma^2 = -94$ dBm. Also, every coherence block consists of $\tau_c = 200$ samples and $\tau_p = 5$ channel uses are reserved for pilot transmission.

Fig. 2 shows the uplink average SE under random UE and AP-RIS locations as the function of the number of RISs T_r for different UEs K. Note that the simulation results and the closed-form solution do not exactly match due to channel spatial correlation. It is clear that for a fixed T_r, the average SE decreases with K increasing. When K is a constant, the average SE increases with the increases of T_r. This reveals that better communication performance can be achieved by increasing the number of RISs in RISs-aided CF massive MIMO system as the increasing number of RIS can effectively improve the communication link strength between transceivers. Besides, the increases in Rician factor enhance the strength of the LoS component and improve the system performance.

Fig. 3 shows the impact on the uplink average SE of the RIS-aided CF system versus different number of elements L in each RIS. The results show that the system performance can be improved by increasing the number of RIS elements, due to the improved beamforming capability of each RIS. On the other hand, when increasing the number of APs, the system performance can also be enhanced. Indeed, the adopted de-centralized control approach can avoid extremely poor communication performance caused by long communication distance between a UE and a AP.

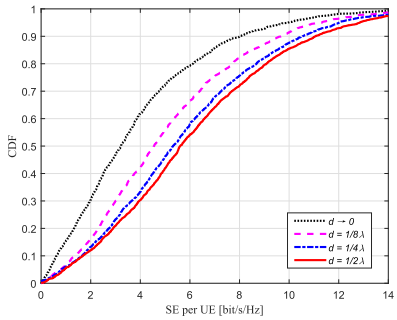

Fig. 4. CDF of SE per UE for $M = 50$, $K = 10$, $L = 64$ with different d_{V}.

Fig. 4 shows the CDF of the SEs under different spatial correlation matrix $\mathbf{R}$. When the spacing between two elements is $d_{\mathrm{V}} = \frac{1}{2}\lambda$, SE achieves the best performance. Also, we observe that the SE decreases as the physical size of each element of the RIS decreases. In fact, changing the element spacing introduces a significant impact on the correlation matrix $\mathbf{R}$ in the denominator of (21), which is related to the characteristics of sinc function. The result provides an insightful reference to design the physical structure of RIS.

V. Conclusion

In this paper, we investigated the uplink performance of the spatially correlated RISs-aided CF massive MIMO systems over Rician fading channel. We derived the closed-form expression for analyzing the uplink SE of the considered system. We found that the SE performance improves with the increase number of RISs or RIS elements. By reasonably designing the inter-distance among RIS elements as at least half wavelength, the deteriorating effect of spatial correlation is notably reduced and hence improves the SE performance. In our future work, we will study the system performance by considering more practical scenarios such as the existence of the AP-UE direct link and the spatial correlation of multi-antenna APs.

Appendix A
Proof of UL SE With MMSE Estimator

This appendix calculates the expected values in (16) and (17). For $m \neq n$ and $k = u$, we obtain

$$\mathbb{E}\left\{\left(v_{mtk}^H g_{mtk}\right)^H \left(v_{ntk}^H g_{ntk}\right)\right\}$$
$$=\hat{p}_k^2\tau_p^2 \mathrm{tr}(\mathbf{\Omega}_{mtk})\mathrm{tr}(\mathbf{\Omega}_{ntk}) + \left|\bar{\mathbf{g}}_{mtk}^H \bar{\mathbf{g}}_{ntk}\right|^2$$
$$+ \hat{p}_k\tau_p \mathrm{tr}(\mathbf{\Omega}_{mtk})\|\bar{\mathbf{g}}_{ntk}\|^2 + \hat{p}_k\tau_p \mathrm{tr}(\mathbf{\Omega}_{ntk})\|\bar{\mathbf{g}}_{mtk}\|^2. \quad (22)$$

Similarly for $m = n$ and $k = u$, we calculate the following equation as

$$\mathbb{E}\left\{\left|\hat{\mathbf{g}}_{mtk}^H \tilde{\mathbf{g}}_{mtk}\right|^2\right\} = \left(\hat{p}_k\tau_p \mathrm{tr}\left(\mathbf{\Omega}_{mtk}\right) + \|\bar{\mathbf{g}}_{mtk}\|^2\right)\mathbf{C}_{mtk}. \quad (23)$$

To calculate $\mathbb{E}\{|\hat{\mathbf{g}}_{mtk}|^4\}$, we rewrite the MMSE estimator in (6) as

$$\hat{\mathbf{g}}_{mtk} = \bar{\mathbf{g}}_{mtk} + \sqrt{\hat{p}_k}\mathbf{R}_{mtk}\mathbf{\Lambda}_{mtk}^{-1}\left(\mathbf{y}_{mtk}^p - \bar{\mathbf{y}}_{mtk}^p\right)$$
$$= \sqrt{\hat{p}_k\tau_p}\mathbf{R}_{mtk}\mathbf{\Lambda}_{mtk}^{-1/2}\mathbf{w} + \bar{\mathbf{g}}_{mtk}, \quad (24)$$

where $\mathbf{w} \sim \mathcal{CN}(0, \mathbf{I})$. After that, we directly compute

$$\mathbb{E}\left\{\left|\hat{\mathbf{g}}_{mtk}\right|^4\right\} = 2\hat{p}_k^2\tau_p^2\mathrm{tr}(\mathbf{\Omega}_{mtk})^2 + 3\hat{p}_k\tau_p\mathrm{tr}\left(\mathbf{\Omega}_{mtk}\right)\bar{\mathbf{g}}_{mtk}^H\bar{\mathbf{g}}_{mtk}$$
$$+ \left(\mathbf{R}_{mtk} - \mathbf{C}_{mtk}\right)\bar{\mathbf{g}}_{mtk}^H\bar{\mathbf{g}}_{mtk} + \left|\bar{\mathbf{g}}_{mtk}^H\bar{\mathbf{g}}_{mtk}\right|^2. \quad (25)$$

Combining (23) and (25) arrives

$$\mathbb{E}\left\{\left(v_{mtk}^H g_{mtk}\right)^H \left(v_{mtk}^H g_{mtk}\right)\right\} = \mathbb{E}\left\{\left|\hat{\mathbf{g}}_{mtk}\right|^4\right\} + \mathbb{E}\left\{\left|\hat{\mathbf{g}}_{mtk}^H\tilde{\mathbf{g}}_{mtlk}\right|^2\right\}$$
$$= \hat{p}_k\tau_p\mathrm{tr}\left(\mathbf{R}_{mtk}\mathbf{\Omega}_{mtk}\right) + \hat{p}_k^2\tau_p^2\mathrm{tr}(\mathbf{\Omega}_{mtk})^2$$
$$+3\hat{p}_k\tau_p\mathrm{tr}\left(\mathbf{\Omega}_{mtk}\right)\bar{\mathbf{g}}_{mtk}^H\bar{\mathbf{g}}_{mtk} + \mathbf{R}_{mtk}\bar{\mathbf{g}}_{mtk}^H\bar{\mathbf{g}}_{mtk} + \left|\bar{\mathbf{g}}_{mtk}^H\bar{\mathbf{g}}_{mtk}\right|^2. \quad (26)$$

Putting all the equations together for $k = u$, we can obtain (16). For $m = n$ and $u \in \mathcal{P}_k \backslash \{k\}$ using the method in [22], we have

$$\mathbb{E}\left\{\left|\hat{\mathbf{g}}_{mtk}^H\tilde{\mathbf{g}}_{mtu}\right|^2\right\} = \left(\hat{\mathbf{p}}_k\tau_p\mathrm{tr}\left(\mathbf{\Omega}_{mtk}\right) + \|\bar{\mathbf{g}}_{mtk}\|^2\right)\mathbf{C}_{mtu}, \quad (27)$$

$$\mathbb{E}\left\{\left|\hat{\mathbf{g}}_{mtk}^H\hat{\mathbf{g}}_{mtu}\right|^2\right\} = 2\hat{p}_k\tau_p\mathbf{R}_{mtk}^2\mathbf{\Lambda}_{mtk}^{-1}\left(\mathbf{R}_{mtu} - \mathbf{C}_{mtu}\right)$$
$$+ \hat{p}_k\tau_p\mathrm{tr}\left(\mathbf{R}_{mtk}\mathbf{\Lambda}_{mtk}^{-1}\mathbf{R}_{mtk}\right)\bar{\mathbf{g}}_{mtu}^H\bar{\mathbf{g}}_{mtu}$$
$$+ \left(\mathbf{R}_{mtu} - \mathbf{C}_{mtu}\right)\bar{\mathbf{g}}_{mtk}^H\bar{\mathbf{g}}_{mtk} + \left|\bar{\mathbf{g}}_{mtk}^H\bar{\mathbf{g}}_{mtu}\right|^2$$
$$+ 2\sqrt{\hat{p}_k\hat{p}_u}\tau_p\mathbf{R}_{mtk}\mathbf{\Lambda}_{mtk}^{-1}\mathbf{R}_{mtu}\bar{\mathbf{g}}_{mtk}^H\bar{\mathbf{g}}_{mtu}. \quad (28)$$

Then, we obtain

$$\mathbb{E}\left\{\left|v_{mtk}^H g_{mtu}\right|^2\right\} = \mathbb{E}\left\{\left|\hat{\mathbf{g}}_{mtk}^H\hat{\mathbf{g}}_{mtu}\right|^2\right\} + \mathbb{E}\left\{\left|\hat{\mathbf{g}}_{mtk}^H\tilde{\mathbf{g}}_{mtu}\right|^2\right\}$$
$$= \hat{p}_k\tau_p\mathrm{tr}\left(\mathbf{\Omega}_{mtk}\mathbf{R}_{mtu}\right) + \hat{p}_k\tau_p\mathrm{tr}\left(\mathbf{\Omega}_{mtk}\right)\|\bar{\mathbf{g}}_{mtu}\|^2$$
$$+ \mathrm{tr}\left(\mathbf{R}_{mtu}\right)\|\bar{\mathbf{g}}_{mtk}\|^2 + \left|\bar{\mathbf{g}}_{mtk}^H\bar{\mathbf{g}}_{mtu}\right|^2$$
$$+ \begin{cases} \hat{p}_k\hat{p}_u\tau_p^2\mathrm{tr}\left(\mathbf{\Omega}_{mtk}\right)\mathrm{tr}\left(\mathbf{\Omega}_{mtu}\right) \\ +2\sqrt{\hat{p}_k\hat{p}_u}\tau_p\mathbf{R}_{mtk}\mathbf{\Lambda}_{mtk}^{-1}\mathbf{R}_{mtu}\bar{\mathbf{g}}_{mtk}^H\bar{\mathbf{g}}_{mtu}, & u \in \mathcal{P}_k\backslash\{k\} \\ 0, & u \notin \mathcal{P}_k. \end{cases} \quad (29)$$

Substituting the above results into (11) and the results for the UL SE follow immediately.

REFERENCES

[1] J. Zhang *et al.*, "RIS-aided next-generation high-speed train communications: Challenges, solutions, and future directions," *IEEE Wireless Commun.*, vol. 28, no. 6, pp. 145–151, Dec. 2021.

[2] Q. Wu and R. Zhang, "Towards smart and reconfigurable environment: Intelligent reflecting surface aided wireless network," *IEEE Commun. Mag.*, vol. 58, no. 1, pp. 106–112, Jan. 2020.

[3] E. Basar, "Reconfigurable intelligent surface-based index modulation: A new beyond MIMO paradigm for 6G," *IEEE Trans. Commun.*, vol. 68, no. 5, pp. 3187–3196, May 2020.

[4] J. Zhang, E. Björnson, M. Matthaiou, D. W. K. Ng, H. Yang, and D. J. Love, "Prospective multiple antenna technologies for beyond 5G," *IEEE J. Sel. Areas Commun.*, vol. 38, no. 8, pp. 1637–1660, Aug. 2020.

[5] S. Chen, J. Zhang, J. Zhang, E. Björnson, and B. Ai, "A survey on user-centric cell-free massive MIMO systems," *Digit. Commun. Netw.*, 2021.

[6] J. Zheng, J. Zhang, and B. Ai, "UAV communications with WPT-aided cell-free massive MIMO systems," *IEEE J. Sel. Areas Commun.*, vol. 39, no. 10, pp. 3114–3128, Oct. 2021.

[7] S. Chen, J. Zhang, E. Björnson, J. Zhang, and B. Ai, "Structured massive access for scalable cell-free massive MIMO systems," *IEEE J. Sel. Areas Commun*, vol. 39, no. 4, pp. 1086–1100, Apr. 2021.

[8] Y. Xu, H. Xie, Q. Wu, C. Huang, and C. Yuen, "Robust max-min energy efficiency for RIS-aided HetNets with distortion noises," *IEEE Trans. Commun.*, vol. 70, no. 2, pp. 1457–1471, Feb. 2022.

[9] E. Shi *et al.*, "Wireless energy transfer in RIS-aided cell-free massive MIMO systems: Opportunities and challenges," *IEEE Commun. Mag.*, vol. 60, no. 3, pp. 26–32, Mar. 2022.

[10] B. Di, H. Zhang, L. Song, Y. Li, Z. Han, and H. V. Poor, "Hybrid beamforming for reconfigurable intelligent surface based multi-user communications: Achievable rates with limited discrete phase shifts," *IEEE J. Sel. Areas Commun.*, vol. 38, no. 8, pp. 1809–1822, Aug. 2020.

[11] M. Di Renzo *et al.*, "Smart radio environments empowered by reconfigurable intelligent surfaces: How it works, state of research, and the road ahead," *IEEE J. Sel. Areas Commun.*, vol. 38, no. 11, pp. 2450–2525, Nov. 2020.

[12] M. Bashar, K. Cumanan, A. G. Burr, P. Xiao, and M. Di Renzo, "On the performance of reconfigurable intelligent surface-aided cell-free massive MIMO uplink," in *Proc. IEEE Glob. Commun. Conf.*, 2020, pp. 1–6.

[13] Y. Zhang, B. Di, H. Zhang, J. Lin, Y. Li, and L. Song, "Reconfigurable intelligent surface aided cell-free MIMO communications," *IEEE Wireless Commun. Lett.*, vol. 10, no. 4, pp. 775–779, Apr. 2021.

[14] E. Björnson and L. Sanguinetti, "Rayleigh fading modeling and channel hardening for reconfigurable intelligent surfaces," *IEEE Wireless Commun. Lett.*, vol. 10, no. 4, pp. 830–834, Apr. 2021.

[15] T. Van Chien, H. Q. Ngo, S. Chatzinotas, M. Di Renzo, and B. Ottersten, "Reconfigurable intelligent surface-assisted cell-free massive MIMO systems over spatially-correlated channels," *IEEE Trans. Wireless Commun.*, to be published, doi: 10.48550/arXiv.2104.08648.

[16] J. Zhang, H. Du, Q. Sun, B. Ai, and D. W. K. Ng, "Physical layer security enhancement with reconfigurable intelligent surface-aided networks," *IEEE Trans. Inf. Forensics Secur.*, vol. 16, pp. 3480–3495, 2021.

[17] L. Yang, F. Meng, J. Zhang, M. O. Hasna, and M. D. Renzo, "On the performance of RIS-assisted dual-hop UAV communication systems," *IEEE Trans. Veh. Technol.*, vol. 69, no. 9, pp. 10 385–10 390, Sep. 2020.

[18] B. Al-Nahhas, M. Obeed, A. Chaaban, and M. J. Hossain, "RIS-aided cell-free massive MIMO: Performance analysis and competitiveness," in *Proc. IEEE Int. Conf. Commun. Workshops*, 2021, pp. 1–6.

[19] J. Zhang, J. Zhang, D. W. K. Ng, S. Jin, and B. Ai, "Improving sum-rate of cell-free massive MIMO with expanded compute-and-forward," *IEEE Trans. Signal Process.*, vol. 70, pp. 202–215, 2022.

[20] J. Zhang, J. Zhang, E. Björnson, and B. Ai, "Local partial zero-forcing combining for cell-free massive MIMO systems," *IEEE Trans. Commun.*, vol. 69, no. 12, pp. 8459–8473, Dec. 2021.

[21] S. M. Kay, *Fundamentals of Statistical Signal Processing: Estimation Theory*, Englewood Cliffs, NJ, USA: Prentice-Hall, 1993.

[22] Ö Özdogan, E. Björnson, and J. Zhang, "Performance of cell-free massive MIMO with rician fading and phase shifts," *IEEE Trans. Wireless Commun.*, vol. 18, no. 11, pp. 5299–5315, Nov. 2019.

[23] Ö. T. Demir, E. Björnson, and L. Sanguinetti, "Foundations of user-centric cell-free massive MIMO," *Found. Trends Signal Process.*, vol. 14, no. 3/4, pp. 162–472, 2021.

[24] H. Q. Ngo, A. Ashikhmin, H. Yang, E. G. Larsson, and T. L. Marzetta, "Cell-free massive MIMO versus small cells," *IEEE Trans. Wireless Commun.*, vol. 16, no. 3, pp. 1834–1850, Mar. 2017.